Adsorption (2011) 17: 159–170
DOI 10.1007/s10450-010-9299-x

Optimizing the separation of gaseous enantiomers by simulated moving bed and pressure swing adsorption

Jason Bentley · Qinglin Huang · Yoshiaki Kawajiri · Mladen Eic · Andres Seidel-Morgenstern

Received: 15 May 2010 / Accepted: 19 November 2010 / Published online: 7 December 2010

Abstract The resolution of racemic gas mixtures by simulated moving bed (SMB) and pressure swing adsorption (PSA) is investigated by dynamic simulation and optimization. Enantiomer separation of inhalation anesthetics is important because there is evidence that the purified enantiomers may have different pharmacological properties than the racemate. The model parameters reported in an experimental investigation performed elsewhere are used to study the feasibility of this separation using SMB and PSA configurations. Both processes were modeled in gPROMS® as systems of differential algebraic equations. Operating conditions are optimized such that the feed throughput and product recovery for each process were maximized subject to equal constraints on the pressures and superficial gas velocities. SMB was found to be capable of resolving racemic feed mixtures with purity and recovery exceeding 99%. On the other hand, PSA was also able to provide a single purified enantiomer with low recovery of about 30% which may limit its application to enantiomer separation. Nevertheless, PSA consumes less desorbent, and achieves higher throughput at the sacrifice of lower recovery.

J. Bentley · Y. Kawajiri (✉)
School of Chemical and Biomolecular Engineering, Georgia Institute of Technology, Atlanta, GA 30332, USA
e-mail: ykawajiri@chbe.gatech.edu

Q. Huang · M. Eic
Department of Chemical Engineering, University of New Brunswick, Frederickton, NB E3B 5A3, Canada

A. Seidel-Morgenstern
Max Planck Institute for Dynamics of Complex Technical Systems, Sandtorstr. 1, 39106, Magdeburg, Germany

A. Seidel-Morgenstern
Otto-von-Guericke-Universität, 39016, Magdeburg, Germany

Keywords Optimization · SMB · PSA · Adsorption · Enantiomer separation · Enflurane

1 Introduction

The resolution of racemates, one-to-one mixtures of molecules that have the same chemical formula and covalent bonds but whose atoms have different spatial orientations, is a particularly interesting problem. About one-third of all synthetic drugs are marketed as racemates, despite the fact that drug receptors may differentiate between stereoisomers in various ways, such that binding likely favors one orientation over another (Nau and Strichartz 2002). Some of these stereoisomers are more specifically called enantiomers if their three-dimensional projections are non-superimposable. In the past decade, there have been numerous studies that indicate the enantiomers of biologically active molecules have measurable differences in their toxicity and metabolism in the human body (Aboul-Enein and Abou-Basha 1997). More specifically, the mechanism of anesthetic action for fluorinated volatile anesthetics needs to be investigated further in order to design safer general anesthetics with pure enantiomers (Aboul-Enein et al. 2000). Enabling such research is the primary motivation for the present work.

About 28 million people undergo surgery and general anesthesia in the U.S. annually. Based on a recent study of anesthesia mortality in the U.S., it was found that 2,211 people died from complications in anesthesia from 1999–2005 (Li et al. 2009). Thus, anesthesia is a leading cause of death during surgery and leaves room for improvement.

Some investigations of volatile anesthetic compounds have shown that purified enantiomers may have better pharmacological properties compared to the racemate. For example, isoflurane has been studied by Hall et al. (1994)

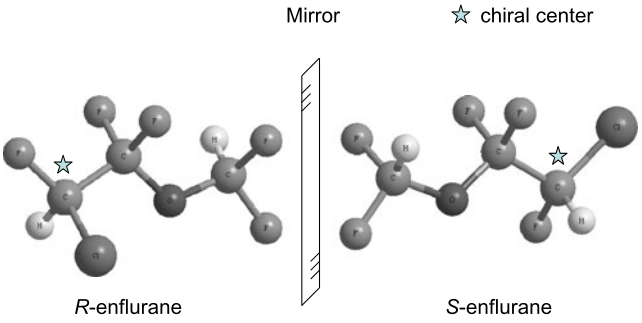

Fig. 1 Chemical structures of enflurane as an example of a chiral inhalation anesthetic, (isoflurane and desflurane are also common fluorinated anesthetics that have similar structures)

and Harris et al. (1994). However, the results of such studies are inconclusive because pure enantiomers are so scarce that only a few animal tests could be performed (Nau and Strichartz 2002; Eger et al. 1997). Hence, there is a need for increased production of pure enantiomers of volatile anesthetics to substantiate these claims. Enflurane, a structural isomer of isoflurane, is another volatile anesthetic with a chiral center that requires further investigation (Fig. 1). One study showed that the metabolism of *R*-enflurane was twice that of *S*-enflurane in the liver, indicating that *R*-enflurane is less toxic than the racemate (Garton et al. 1995). Thus, it may be possible to improve the safety of general anesthesia by employing an enantiomerically purified anesthetic.

The chiral separation of enflurane and other inhalation anesthetics has been demonstrated experimentally (Meinwald et al. 1991) using capillary chromatography, and the original separation protocol was improved upon using a gas chromatographic simulated moving bed (SMB) process (Juza et al. 1998; Biressi et al. 2000, 2002). Small particles of octakis(3-*O*-butanoyl-2,6-di-*O*-*n*-pentyl)-γ-cyclodextrin (γ-CD) were used as the adsorbent, first analyzed by König et al. (1989), which requires a careful synthesis and is rather expensive. *R*- and *S*-enflurane have a slight but exploitable difference in affinity using this chiral adsorbent. The separation factor is about 1.5 at 33°C.

A SMB process exploits multiple columns connected in series where port switching occurs between columns to simulate the countercurrent flow of the stationary phase (Broughton and Gerhold 1961). Descriptions of the SMB process and the role of each adsorption zone can be found elsewhere (for example, Ganetsos and Barker 1993). In this work, a classical four-column four-zone SMB configuration (1,1,1,1) was employed characterized by a closed-loop, such that all of the gas flowing out of the last column in the series passes through a compressor and is recycled to the beginning of the loop (Fig. 2). This represents a base-case design of the SMB process for this study. Significant optimization work has been performed by others to find optimal liquid phase SMB configurations (e.g. Zhang et al. 2004; Mota et al. 2007; Kawajiri and Biegler 2008).

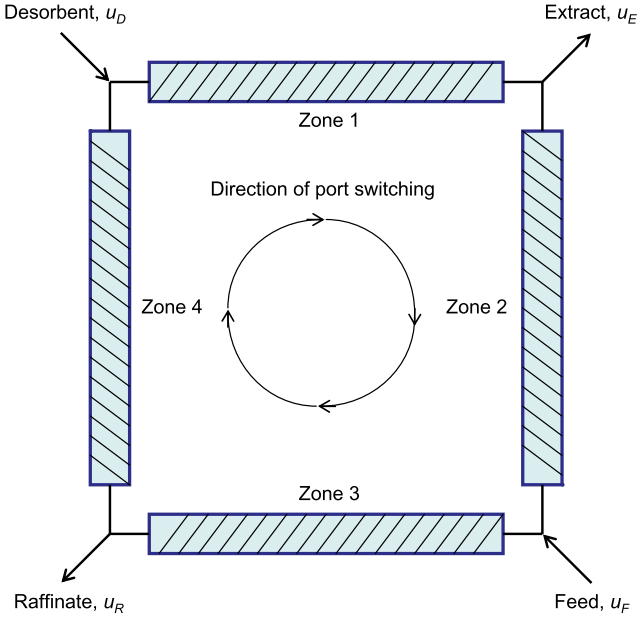

Fig. 2 Schematic of four-zone (1, 1, 1, 1) SMB closed-loop configuration. At the current step, the zone number corresponds directly to the column number (i.e. Column 1 is in Zone 1), and at $t = t_{\text{step}}$ the ports switch position in the direction of mobile phase flow

A typical SMB process consists of the following steps. At a specified time, called t_{step}, the inlet and outlet ports switch such that each flow is transferred from the previous column to the adjacent column. For example, from the above schematic, at $t = t_{\text{step}}$, u_D and u_E are transferred from Column 1 to Column 2, and likewise u_F and u_R are transferred from Column 3 to Column 4. In addition, the stream exiting Column 1 is now diverted to the gas compressor and the stream exiting Column 4 is sent to Column 1. One switching interval is called a step, and four steps are called a cycle.

For the purification of pharmaceutical molecules most SMB processes have been developed applying liquid mobile phases (Schmidt-Traub 2005). In comparison, there are less applications of SMB technology for gas phase separations (Storti et al. 1992; Gomes et al. 2009). There are also applications of SMB in supercritical fluid separations where typically CO_2 is utilized as a solvent (Perrut 1994). In the case considered here, i.e., the separation of the enantiomers of enflurane (or other volatile anesthetics), the chiral separation has been performed in the gas phase where the racemate is diluted in nitrogen. To the best of our knowledge this is the only proven continuous process for achieving enantiomerically pure enfluranes. However, pressure swing adsorption (PSA) may be a viable alternative because it also operates continuously and is capable of purifying gas components with differing affinity for the adsorbent. Although, to date enantiomer separation has not been investigated using PSA alone, it has been reported that SMB may be operated at variable pressure conditions in the adsorption bed

(Rao et al. 2005), or when assisted by a pressure swing could achieve complete enantiomer separation with a noticeable reduction in desorbent consumption over the SMB system by itself (Kostroski and Wankat 2008). In general, there are a number of combinations of gas adsorption processes that merit further research. Indeed, there exist other configurations of adsorption columns with dedicated port switchings and pressure swing steps that have not yet been investigated systematically (e.g. LaCava and McKeigue 1996; Cheng and Wilson 2001).

In the present work, the PSA operation is investigated by dynamic simulation and optimization based on the same system parameters used in the experimental SMB work of Juza et al. (1998) and Biressi et al. (2000, 2002). PSA is based on changing the total pressure in an adsorption column in order to manipulate the elution of the gas phase components. It may be operated with multiple columns in parallel, as well as with numerous operation steps in a cycle. A more detailed description of PSA is given by Ruthven et al. (1994). In this work, a base-case design of a single column with 4 elementary steps was considered, and each step is defined in Fig. 3. A PSA cycle consists of these 4 steps.

The dynamic simulation and optimization of gas phase SMB and PSA processes have been performed by various researchers recently. Ko et al. (2003) worked on the optimization of PSA for CO_2 sequestration from flue gas. Mota et al. (2007) reported optimal SMB configurations and operating conditions for the separation of CH_4 from CO_2. Huang et al. (2008) showed that PSA could be optimized to separate H_2 from CH_4. Likewise, Gomes et al. (2009) investigated the feasibility of using SMB for the separation of propane from propylene using a numerical optimization scheme. Kostroski and Wankat (2008) demonstrated the enantiomer separation of enflurane with their hybrid SMB/PSA system along with numerical simulation results. This research provides insight about how to choose the operating conditions for the process in question. Nevertheless, no systematic study based on dynamic optimization has addressed concepts to select an adsorption process out of rivaling options until now.

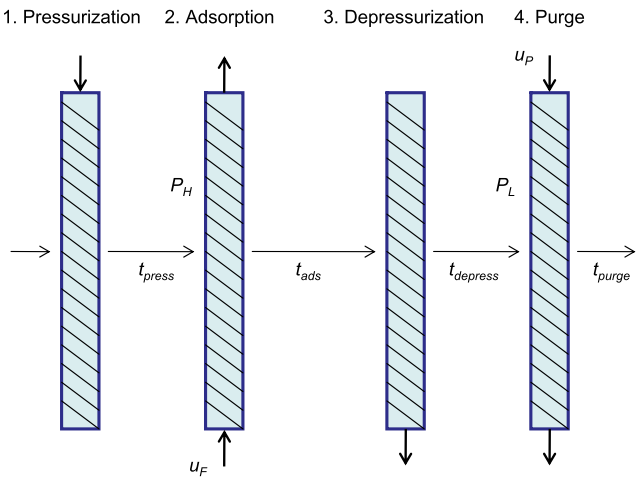

Fig. 3 Schematic of 4-step PSA cycle: 1—pressurization with desorbent supplied until high pressure for duration of t_{press}; 2—adsorption at high pressure with feed supplied and raffinate collected for duration of t_{ads}; 3—depressurization until atmospheric pressure with extract wasted for duration of t_{depress}; 4—purge with desorbent supplied at atmospheric pressure and extract collected for duration of t_{purge}

In this work, dynamic simulations and optimizations of SMB and PSA processes are performed to find the optimal operating conditions for the enantiomer separation of enflurane. The operating parameters to be optimized include step times, pressures, and flow rates, at which SMB and PSA are the most productive while achieving an enantiomerically pure product. From these solutions, the two processes can be compared regarding productivity and desorbent consumption.

2 Methodology

2.1 Gas adsorption column model

The modeling of SMB and PSA processes typically begins with the description of a single fixed-bed or column. The column packing is assumed to be homogeneous, and the gas phase is assumed to obey dispersed plug flow behavior at the selected operating conditions such that any spatially dependent variable in the column, such as concentration, varies with only one spatial dimension, the axial position. In addition, isothermal operation is assumed because the feed is diluted significantly in a carrier gas and the heat of adsorption can be neglected. These assumptions are typically made for trace gas phase systems (Ruthven et al. 1994; Gomes et al. 2009).

With regard to mass balances, both a component mass balance and an overall mass balance were implemented to capture the dynamics of convection and adsorption in the column. The ideal gas law was assumed because the total pressure and feed concentration of enflurane are relatively low. Further, we assumed a negligible pressure drop in the columns at the selected operating conditions. This assumption is frequently used in modeling gas phase chromatography (Huang et al. 2008; Ruthven et al. 1994). Hence, the component mass balance is given by the partial differential equation:

$$u(z,t)\frac{\partial y_i(z,t)}{\partial z} + y_i(z,t)\frac{\partial u(z,t)}{\partial z} + \varepsilon^*\frac{\partial y_i(z,t)}{\partial t} + (1-\varepsilon^*)\frac{RT}{P(t)}\frac{\partial q_i(z,t)}{\partial t} = 0$$
$$i = 1, 2, \ldots, n \qquad (1)$$

where $u(z,t)$ is the superficial velocity of the gas phase, $y_i(z,t)$ is the gas phase mole fraction of the ith component, z denotes the axial position, ε^* is the overall porosity, t denotes the time, R is the gas constant, T is the operating temperature, $P(t)$ is the total pressure, $q_i(z,t)$ is the molar solid phase concentration of the ith component, and n is the number of adsorbable components. A constant column pressure model was considered for the overall mass balance in the SMB process as well as the adsorption and purge steps of PSA (Fig. 3, steps 2 and 4):

$$\frac{\partial u(z,t)}{\partial z} + (1-\varepsilon^*)\frac{RT}{P(t)}\sum_{i=1}^{n}\frac{\partial q_i(z,t)}{\partial t} = 0$$
$$i = 1,2,\ldots,n \tag{2}$$

For the pressurization and depressurization steps of PSA (Fig. 3, steps 1 and 3), where the column pressure is dynamic, the variable column pressure model was used:

$$\frac{\partial u(z,t)}{\partial z} + \varepsilon^*\frac{1}{P(t)}\frac{\partial P(t)}{\partial t} + (1-\varepsilon^*)\frac{RT}{P(t)}\sum_{i=1}^{n}\frac{\partial q_i(z,t)}{\partial t} = 0$$
$$i = 1,2,\ldots,n \tag{3}$$

where the total pressure in the column is assumed to change linearly with time. The inclusion of the overall mass balance is necessary for gas phase systems because the fluid is compressible, and during adsorption the local velocity of the fluid varies.

With regard to mass transfer, the linear driving force (LDF) model was implemented. The LDF model was chosen because it is realistic to assume a finite mass transfer resistance in the boundary layer of the adsorbent particles. Also, this model is frequently used in the modeling of gas phase adsorption processes (Huang et al. 2008; Ruthven et al. 1994; Nilchan and Pantelides 1998). The rate of mass transfer is approximated as a first-order linear differential equation using a LDF model in the loadings:

$$\frac{\partial q_i(z,t)}{\partial t} = k_i\left(q_i^{eq}(z,t) - q_i(z,t)\right) \tag{4}$$

where k_i is the mass transfer coefficient of the ith component, $q_i^{eq}(z,t)$ is the molar solid phase concentration of the ith component in equilibrium with the gas phase, and $q_i^{eq}(z,t) - q_i(z,t)$ represents the mass transfer resistance in the solid phase. The axial dispersion and mass transfer coefficients contribute to the column efficiency, but the axial dispersion term was neglected. Therefore, all band broadening effects are captured by (4) and k_i. This simplifies the modeling of the adsorption processes because the boundary conditions do not take a differential form.

With regard to thermodynamics, it was assumed that the affinity between the adsorbent particles and the gas phase components reduces to a linear isotherm as described by Henry's law:

$$q_i^{eq}(z,t) = H_i(T)\frac{P(t)y_i(z,t)}{RT} \tag{5}$$

where $H_i(T)$ is the temperature dependent Henry's law constant of the ith component. The use of Henry's law is justified because the target compounds are assumed to be present in minor concentrations. This linear model has been used often to quantify thermodynamics in diluted systems.

2.2 SMB model

In order to obtain the time evolution of the internal profiles in the column series, the system of algebraic and partial differential equations outlined above must be solved numerically. Equations (1)–(2) specifically require a set of boundary and initial conditions. The boundary conditions for the jth column are illustrated in Fig. 4 as suggested in the modeling approach of Dünnebier and Klatt (2000). Note that the outlet variables from the previous column are equal to the inlet variables of the next column according to the equations:

$$P_{\text{out}}^{j}(t) = P^{j+1}(t) \quad j = 1,2,\ldots,N_{\text{column}}-1 \tag{6a}$$
$$P_{\text{out}}^{N_{\text{column}}}(t) = P^{1}(t) \tag{6b}$$
$$u_{\text{out}}^{j}(t) = u_{in}^{j+1}(t) \quad j = 1,2,\ldots,N_{\text{column}}-1 \tag{6c}$$
$$u_{\text{out}}^{N_{\text{column}}}(t) = u_{in}^{1}(t) \tag{6d}$$
$$y_{i,\text{out}}^{j}(t) = y_{i,in}^{j+1}(t) \quad j = 1,2,\ldots,N_{\text{column}}-1 \tag{6e}$$
$$y_{i,\text{out}}^{N_{\text{column}}}(t) = y_{i,in}^{1}(t) \tag{6f}$$

where N_{column} is the number of columns. In this model there are four columns and four zones. In Zone 1 the desorbent is supplied and the extract is withdrawn while in Zone 3 the feed is supplied and the raffinate is withdrawn. After duration of t_{step} the zones switch from one column to the next in the direction of mobile phase flow.

The initial conditions must be specified for the mole fraction of the ith component in the gas phase as well as the concentration of the ith component in the solid phase. For the start-up simulation, it is assumed that the gas adsorption columns are initially filled with desorbent, such that the concentration of the adsorbable species is zero everywhere except at the boundary condition:

$$y_i^j(z,0) = 0 \quad 0 < z \le L,\ j = 1,2,\ldots,N_{\text{column}} \tag{7a}$$
$$q_i^j(z,0) = 0 \quad 0 \le z \le L,\ j = 1,2,\ldots,N_{\text{column}} \tag{7b}$$

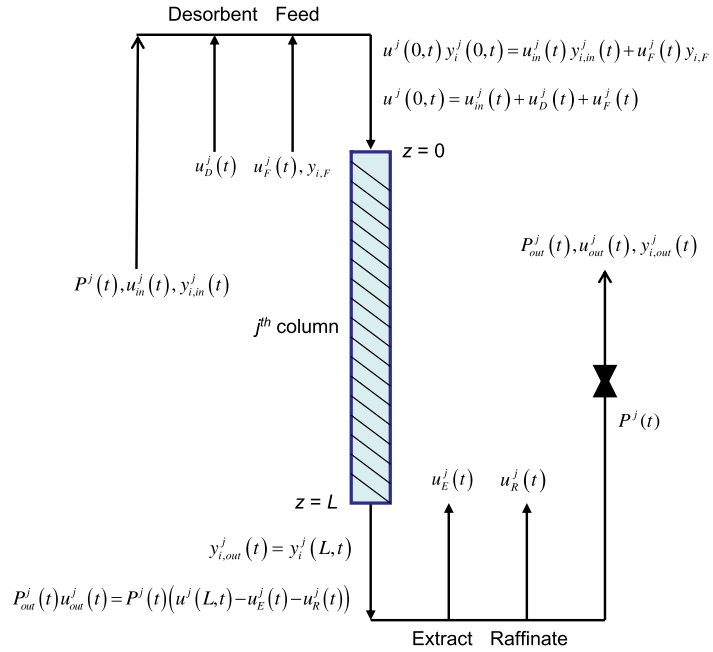

Fig. 4 Illustration of boundary conditions for the SMB process in the jth column. The gas phase mole fraction and superficial velocity are distributed variables such that the first ordinate is the axial position and the second ordinate is the time. At $t = t_{\text{step}}$ all the variables are switched to match the port switching on the jth column

and the SMB process is simulated until the cyclic steady state (CSS) condition is reached. The CSS condition was verified by plotting the profiles of the time-dependent variables, such as raffinate purity, over multiple steps and confirming that the profiles remain unchanged. Each step of the SMB process is identical once the CSS condition has been reached, and thus it is possible to run a one-step simulation, where (7a)–(7b) are initialized with the CSS internal profiles (see Sect. 2.6 on the optimization problem formulation) and the process is simulated for duration of t_{step}. This definition is important for the optimization strategy.

2.3 PSA model

To obtain the time evolution of the concentration profiles in PSA, the model (1)–(3) need to be solved numerically with a set of boundary and initial conditions. The boundary conditions for the 4-step PSA process are illustrated in Fig. 5 according to the operation strategy discussed previously in Fig. 2 from Sect. 1. This description of the process is similar to the one used by Ko et al. (2003).

The initial conditions must be specified for the mole fraction of the ith component in the gas phase as well as the concentration of the ith component in the solid phase. For the start-up simulation, it is assumed that the gas adsorption column is initially filled with desorbent, such that the concentration of the adsorbable species is zero everywhere:

$$y_i(z,0) = 0 \quad 0 \le z \le L \tag{8a}$$

$$q_i(z,0) = 0 \quad 0 \le z \le L \tag{8b}$$

and the PSA process is simulated until the CSS condition is reached. Every cycle of the PSA process is identical at the

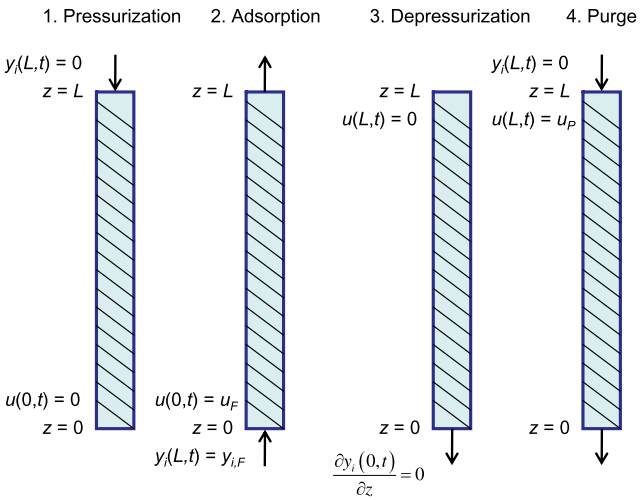

Fig. 5 Illustration of the boundary conditions for the PSA process where the gas phase mole fraction and superficial velocity are distributed variables such that the first ordinate is the axial position and the second ordinate is the time

CSS condition and thus a one-cycle simulation is defined as a process simulation for a single cycle time (t_{cycle}), the sum of the times for each step of the cycle. Equations (8a)–(8b) are initialized with the CSS internal profiles from the start-up simulation. This definition is important in the optimization strategy (see Sect. 2.6 on the optimization problem formulation).

2.4 Numerical solution

The SMB and PSA models were simulated in gPROMS® version 3.2, released by Process Systems Enterprise Lim-

ited in 2009. The models were solved by the method of lines (Schiesser 1991), discretizing the axial domain using the second-order centered finite difference method. Typically, for the conditions introduced below, 100 axial discretization points per column were selected for both SMB and PSA. The difference in the numerical precision of the internal profiles when 50, 100 or 150 axial discretization points are used was checked and was found to be negligible. The number of cycles required to reach CSS was found to be less for the PSA process compared to SMB. The CSS conditions are described in Sect. 2.6 on the optimization problem formulation.

2.5 System parameters

Based on the experimental studies of Juza et al. (1998) and Biressi et al. (2000), the system parameters used for the simulation and optimization of SMB and PSA for the enantiomer separation of enflurane are tabulated below (Table 1). Unless otherwise stated, it is understood that the given values were used in both SMB and PSA models. The particle size of the chiral γ-CD adsorbent was 250 to 350 μm, the overall porosity was measured to be 0.75, and the Darcy's law constant was measured to be 6 bar s m^{-2}. The pressure drop observed in the experimental work was about 1 bar over 8 columns for a total length of 6.4 m (Biressi et al. 2000), and it was assumed that the pressure drop would be negligible in the systems for this study. This assumption is frequently used for modeling gas phase systems (Huang et al. 2008; Ruthven et al. 1994). The Henry's constants for R- and S-enflurane were measured at 306 K and are given in Table 1. The target molecule, R-enflurane, is the less adsorbed component in this separation and is therefore collected in both processes in the raffinate stream. The separation factor is around 1.5. At a temperature of 306 K the vapor pressure of enflurane is about 0.4 bar. The mass transfer coefficients were not directly available for this system; however, the column efficiency was reported in Biressi et al. (2000). A reasonable value for the mass transfer coefficient was chosen based on its consistency with the reported column efficiency, which corresponds to a plate number of approximately 500 (i.e. $k_i = 1$ s^{-1}). A pulse experiment was done in simulation, and it was found that internal profiles were insensitive to the value of k_i.

Table 1 System parameters for the separation of enflurane enantiomers

Parameter	Value
Average adsorbent particle size,[a] d_p [μm]	300
Overall porosity,[a] ε^*	0.75
Henry's law constant for R-enflurane,[b] H_R	118
Henry's law constant for S-enflurane,[b] H_S	175
Mass transfer coefficients, $k_R = k_S$ [s^{-1}]	1
Column diameter,[a] d_c [m]	0.015
Single column length, L [m]	0.4
Number of columns, N_{column}	SMB: 4, PSA: 1
Operating temperature, T [K]	306
Feed mole fractions, $y_{R,F} = y_{S,F}$	0.018

[a]From Biressi et al. (2000)

[b]From Juza et al. (1998)

All of the columns have an internal diameter of 0.015 m that is consistent with the experimental apparatus reported. The SMB process has 4 columns as the most basic 4-zone column configuration. The length of each SMB column was set at 0.4 m and the total length of the system is 1.6 m, while the PSA process has a single column with a length of 0.4 m.

The feed mole fractions were selected to be 0.018 for both R- and S-enflurane, and these are diluted in nitrogen, an inert (non-adsorbed) carrier gas, such that the total mole fraction of enflurane in the feed was 0.036. This value is still small enough to avoid condensation and to justify the application of linear isotherms. This concentration is also consistent with the range of feed concentrations used in the experiments (Biressi et al. 2000).

Nitrogen is employed as desorbent in both SMB and PSA systems at the system pressure such that the only components in each system are R-enflurane, S-enflurane and nitrogen. Nitrogen acts as an inert carrier gas in this case, so the Henry's law constant is set to zero, and there is no competition between nitrogen and the enfluranes for adsorption sites.

2.6 Optimization problem formulation

For both SMB and PSA, we consider a multi-objective optimization: the maximization of both throughput and target recovery.

$$\max \quad \text{Throughput} \tag{9a}$$

$$\max \quad \text{Recovery} \tag{9b}$$

The trade-off of these two objectives is investigated by deterministic dynamic optimization using the ε-constraint method for multi-objective optimization. For SMB, the objective function is the maximization of Throughput and this function is constrained by a minimum raffinate recovery defined in (10a)–(10b) below. The problem is formulated as:

$$\max_{t_{\text{step}}, u^1, u^2, u^3, u^4, P} \quad \text{Throughput} \tag{10a}$$

$$\text{s.t.} \quad \text{Recovery}_1^{\text{Raffinate}} \geq \varepsilon_{\text{Rec}} \tag{10b}$$

where t_{step} is the time between each port-switching step, u^j is the inlet superficial velocity in the jth zone, P is the total

pressure. Throughput is the mass flow rate of the feed, and ε_{Rec} is a minimum raffinate recovery value that is varied to generate a Pareto curve. Again, the inlet superficial velocity, u^j is defined as the velocity of the gas at the location $z = 0$ during a particular step of the SMB cycle. Throughput is not a decision variable, but it is a function of pressure, P multiplied by the difference between u^3 and u^2, because the feed is supplied between Zone 2 and Zone 3. It is important to note that the SMB process has six degrees of freedom. Furthermore, in optimization of SMB, both raffinate purity and recovery requirements can be specified independently, and both constraints are always active at the optimal solution.

On the other hand, we reformulate the multi-objective optimization problem (9a)–(9b) differently, since the reformulation above leads to infeasible optimization problems when ε_{Rec} is high. Here, the objective function for PSA is to maximize the target recovery subject to a minimum throughput constraint. The problem is formulated as:

$$\max_{t_{\text{ads}}, t_{\text{purge}}, u_F, u_P, P_H} \quad \text{Recovery}_1^{\text{Raffinate}} \tag{11a}$$

$$\text{s.t.} \quad \text{Throughput} \geq \varepsilon_{\text{Thr}} \tag{11b}$$

where t_{ads} is the time for the adsorption step, t_{purge} is the time for the purge step, u_F is the superficial velocity of the feed stream, u_P is the velocity of the desorbent stream during the purge step, P_H is the high pressure reached during the pressurization step that is maintained during the adsorption step, Recovery is the percent of R-enflurane recovered in the raffinate stream defined by (13) below, Throughput is the mass flow rate of the feed, which is u_F multiplied by P_H multiplied by the ratio of the adsorption time to the cycle time, and ε_{Thr} is a minimum throughput value that is varied to generate a Pareto curve. To simplify the analysis of the times for the pressurization and depressurization steps, t_{press} and t_{depress} were fixed in the calculations presented below; both at 30 s. Atmospheric pressure was fixed as the pressure for the depressurization and purge steps (P_L). Thus, PSA was considered to have five degrees of freedom.

The separation performance of SMB and PSA was evaluated based on the purity and recovery of the light component defined as:

$$\frac{\int_0^{t^*} u_R(t) y_1(z_R, t)\, dt}{\sum_{i=1}^{n} \int_0^{t^*} u_R(t) y_i(z_R, t)\, dt} = \text{Purity}_1^{\text{Raffinate}} \tag{12}$$

$$\frac{\int_0^{t^*} u_R(t) y_1(z_R, t)\, dt}{\int_0^{t^*} u_F(t) y_1(z_F, t)\, dt} = \text{Recovery}_1^{\text{Raffinate}} \tag{13}$$

where t^* equals t_{step} or t_{ads} for the SMB or PSA processes respectively, $u_R(t)$ is the superficial velocity in the raffinate stream, z_R is the characteristic location of the raffinate port, $u_F(t)$ is the superficial velocity of the feed stream, z_F is the characteristic location of the feed port, and the subscript 1 indicates the target R-enflurane. Both (12)–(13) were applied to the SMB optimization as constraints. The minimum raffinate purity was fixed at 99% and the minimum raffinate recovery was varied according to the epsilon constraint method described above. Equation (12) was a constraint and (13) was the objective function applied to the PSA optimization. Again, the minimum raffinate purity was fixed at 99%.

There are multiple approaches to this optimization problem, as were discussed in Kawajiri and Biegler (2006a). The method of choice for this problem, which allows the simultaneous solution of the optimal operating parameters and internal profiles with a single discretization of the axial domain, is to eliminate the computational cost to integrate the partial differential algebraic equations that describe the transient dynamics before reaching the CSS (Jiang et al. 2003).

These processes never reach a steady state where all the time-dependent variables become constant, but instead they reach a cyclic steady state condition where all the time-dependent variables are equal at the beginning and end of a cycle. An important part of this optimization formulation is the CSS definition because the internal profiles become decision variables, and the CSS condition must be satisfied during normal operation to guarantee the required purity and recovery. Using the LDF model, both the gas and solid phase concentration profiles make up the set of values needed in the CSS definition for SMB:

$$y_i^j(z, 0) = y_i^{j+1}(z, t_{\text{step}}) \quad j = 1, 2, \ldots, N_{\text{column}} - 1 \tag{14a}$$

$$y_i^{N_{\text{column}}}(z, 0) = y_i^1(z, t_{\text{step}}) \tag{14b}$$

$$q_i^j(z, 0) = q_i^{j+1}(z, t_{\text{step}}) \quad j = 1, 2, \ldots, N_{\text{column}} - 1 \tag{14c}$$

$$q_i^{N_{\text{column}}}(z, 0) = q_i^1(z, t_{\text{step}}) \tag{14d}$$

Therefore, the internal profiles in the jth column match the internal profiles in the $(j + 1)$th column at the end of a step, $t = t_{\text{step}}$. This is because SMB repeats identical operations while the components propagate to the columns downstream. On the other hand, the CSS definition for the PSA process can be described as follows:

$$y_i(z, 0) = y_i(z, t_{\text{cycle}}) \tag{15a}$$

$$q_i(z, 0) = q_i(z, t_{\text{cycle}}) \tag{15b}$$

where t_{cycle} is the time for a single PSA cycle, which is the sum of the four times for the individual steps. Thus, the internal profiles are equal at each point in the column at the beginning and end of a cycle.

Both the superficial velocities and pressures were constrained by upper and lower bounds. The aforementioned

constraints were selected to match the experimental conditions used by Biressi et al. (2000, 2002). All upper and lower bounds specified for these decision variables are given in Table 2, and the boundaries are the same for both SMB and PSA as applicable. Identical upper bounds were employed since we assume the same operating equipments are used, such as gas compressors. The lower bounds were set to reasonable values that can be easily realized, and we later confirmed that these lower bounds are always inactive at the optimal solutions.

The optimization problems are also constrained by the component and overall mass balances described in (1)–(3). Due to these PDE constraints, the optimization is dynamic in nature and the Jacobian is obtained from sensitivity equations (Nilchan and Pantelides 1998).

Each optimization problem was initialized with a feasible operating condition which were obtained from simulation in gPROMS®. Then the optimal solutions were found also in gPROMS® using the SRQPD solver for nonlinear programs (Process Systems Enterprise 2009). The optimization algorithm on average converged in two hours depending on the problem size and the processor speed of the computer. More details on the optimization strategy are described in Ko et al. (2003) and Huang et al. (2008).

Table 2 Upper and lower bounds on the decision variables for SMB and PSA

Decision variable	Lower bound	Upper bound
Superficial velocity, u [cm s^{-1}]	0	10.7
Pressure, P [bar]	2	4.5
Step time, t_{step} [s]	10	10000
Cycle time, t_{cycle} [s]	10	10000

3 Results

3.1 Optimized internal profiles for SMB and PSA

Here we only present the results where 99% raffinate purity in *R*-enflurane is achieved. Optimized internal profiles for SMB and PSA are displayed in Figs. 6 and 8 with the corresponding optimized operating conditions in Tables 3 and 4, respectively. The plots show the CSS profiles from simulations using the optimum operating parameters.

In the optimal solution, the maximized throughput is 5.0 g enflurane feed day^{-1} cm^{-3} adsorbent while satisfying 99% raffinate purity and 99% raffinate recovery. The pressure and velocity in Zone 1, where bed regeneration takes place, are both active at the upper bound. These values in Zone 1 are the highest in the SMB unit to facilitate fast desorption. The internal concentration profiles can be seen in Fig. 6 to have a nearly symmetrical shape, which is a characteristic of the linear isotherm. Figure 7 shows the effluent profiles for both enantiomers at the raffinate port during a single step of the SMB cycle. At the CSS condition,

Table 3 SMB operating condition for the simulation of the optimal solution leading to 99% raffinate purity, 99% raffinate recovery and a throughput of 5.0 g enflurane feed day^{-1} cm^{-3} adsorbent

Operating parameter	Value
Step time, t_{step} [s]	181.6
Total pressure, P [bar]	4.5[a]
Velocity in zone 1, u^1 [cm s^{-1}]	10.7[a]
Velocity in zone 2, u^2 [cm s^{-1}]	7.1
Velocity in zone 3, u^3 [cm s^{-1}]	9.1
Velocity in zone 4, u^4 [cm s^{-1}]	6.1

[a]Active upper bound

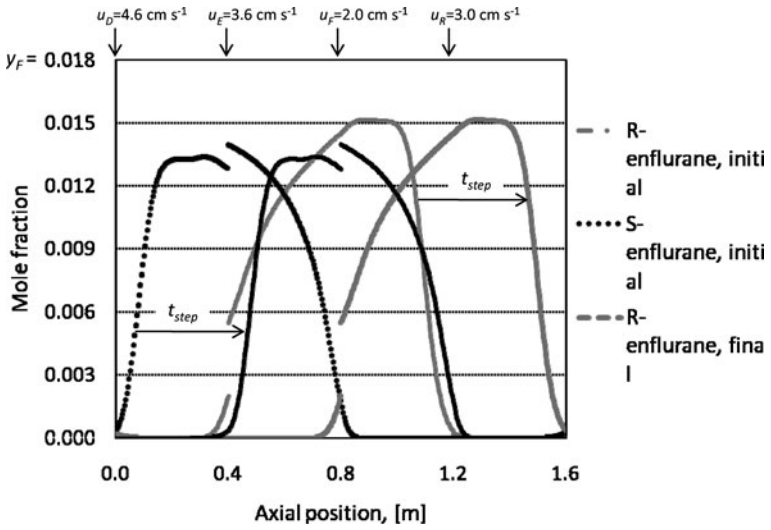

Fig. 6 Internal profiles of *R*- and *S*-enflurane resulting from SMB simulation at the beginning and end of a step with operating condition in Table 3. The feed mole fraction is 0.018. The *horizontal arrows* show the shift in the profile after t_{step}. The *vertical arrows* above the graph show the inlet and outlet flow positions and velocities during the step

this trend is repeated over and over with every step of the process. It can be seen that the unwanted enantiomer pollutes the product just before the switch, thus, 99% raffinate purity is achieved. The average outlet concentration of *R*-enflurane can be estimated by computing the area under the concentration curve and dividing by the step time. This value is about 0.012, which is two-thirds of the feed concentration. The ability to reach a target recovery as high as 99% is a significant advantage for the SMB process.

The optimal operating condition for the PSA process that maximizes the throughput and recovery is shown in Table 4. The maximized raffinate recovery is 27.3% where the throughput is 16.6 g enflurane day^{-1} cm^{-3} adsorbent while achieving 99% raffinate purity. From this result, it is concluded that at the sacrifice of recovery, the PSA process can produce pure *R*-enflurane at a reasonably high throughput. Here, the upper bound on the pressure is active during the adsorption step where it is critical to force the less adsorbed component through the column. Also, the velocity during the purge step is active at the upper bound to minimize the time for purging the column. In Fig. 8 it is shown how over time the *R*-enflurane traverses the column at a faster rate than *S*-enflurane; a consequence of their relative adsorption affinities. Also, *R*-enflurane has a slight overshoot of the feed concentration at the peak of the propagation front. This is due to an incomplete regeneration of the column during purging. The overshoot effect actually contributes to slightly increase the target recovery.

In Fig. 9 it can be seen that at about 750 s, the unwanted component begins to pollute the raffinate stream, and so the adsorption step is ended at the point where 99% raffinate purity is achieved (760 s). The average mole fraction of *R*-enflurane in the raffinate product is about 0.012, assuming the raffinate collection begins at a breakthrough time of about 450 s, which is equal to about two-thirds of the feed concentration. This product concentration is nearly the same

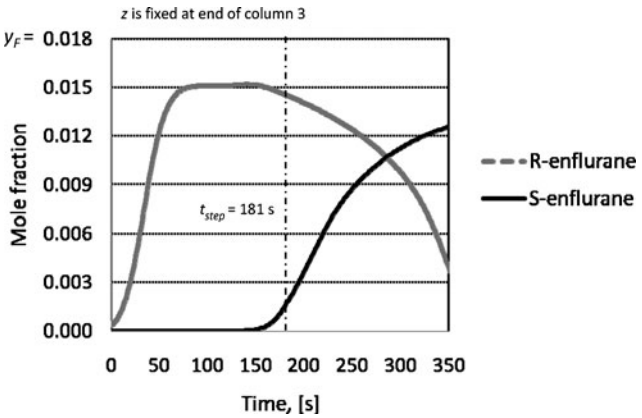

Fig. 7 Mole fraction profiles of *R*- and *S*-enflurane at the end of Column 3 during two steps the of the SMB simulation with operating condition in Table 3. During the step the outlet mole fraction is collected in the raffinate stream. The feed mole fraction is 0.018, and the step time is 181 s

Table 4 PSA operating condition for the simulation of the optimal solution leading to 99% raffinate purity, 16.6 g enflurane feed day^{-1} cm^{-3} adsorbent and 27.3% raffinate recovery

Operating parameter	Value
u_F [cm s^{-1}]	2.2
u_P [cm s^{-1}]	10.7[a]
P_H [bar]	4.5[a]
P_L [bar][b]	1.0
Pressurization time, t_{press} [s][b]	30
Adsorption time, t_{ads} [s]	760
Depressurization time, $t_{depress}$ [s][b]	30
Purge time, t_{purge} [s]	210
Cycle time, t_{cycle} [s]	1030

[a]Active upper bound

[b]Fixed quantity in the optimization

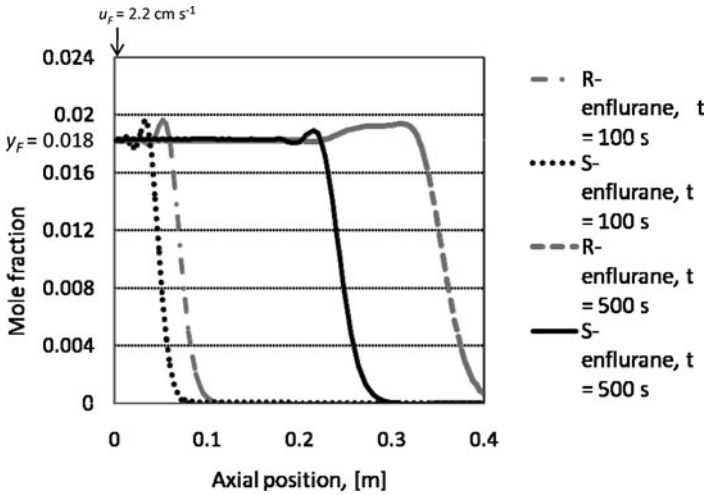

Fig. 8 Internal profiles of *R*- and *S*-enflurane resulting from PSA simulation during the adsorption step of a cycle with operating condition in Table 4. The feed u_F is supplied at the column entrance and the feed mole fraction is 0.018. The profiles are plotted at $t = 100$ and 500 s where $t_{ads} = 760$ s

as that of the SMB process. Nevertheless, the low value of 27.3% raffinate recovery is a disadvantage. We believe this is because both enantiomers of enflurane are adsorbed relatively strongly to the stationary phase, and their concentrations do not attain a high degree of separation from each other.

3.2 Comparison of SMB and PSA optimal solutions

The optimal solutions for the SMB and PSA processes are plotted on a Pareto curve in Fig. 10 showing the enflurane throughput depending on raffinate recovery. It should be mentioned again that in all optimal solutions 99% raffinate purity was achieved, and therefore the target molecule, *R*-enflurane can be produced at this purity.

It can be seen that much lower recovery was obtained from PSA in comparison to SMB; PSA suffers more from the low selectivity (∼1.5) between *R*- and *S*-enflurane as well as their significant affinities for the stationary phase. For the simplified PSA configuration analyzed here, a majority of *R*-enflurane is adsorbed during the adsorption step, and most of the adsorbed components are, in the classical configuration, vented out as waste in the following depressurization and purge steps, rendering low recovery. Whereas for SMB, the adsorbed *R*-enflurane is desorbed by nitrogen and then re-sorbed or eluted as raffinate product in the following zones.

The trade-off between the maximized throughput and target recovery requirements is investigated and shown in Fig. 10. Interestingly, the optimal recovery of PSA appears to have a linear dependence on the throughput. Even when the throughput is decreased to 3.8 g enflurane feed day^{-1} cm^{-3} adsorbent, the recovery increased only to 29.9%. From this result, it can be concluded that for highly valuable products such as chiral anesthetic compounds, 4-zone SMB is more advantageous than the standard 4-step PSA.

However, Fig. 11 demonstrates a key advantage in the PSA process, which is reduced desorbent consumption. In the SMB process, desorbent is supplied continuously at the highest flow rate to facilitate fast desorption and regenerate the column in Zone 1. This causes the ratio of desorbent to feed flow rate, D/F to be relatively large. On the other hand, the PSA process requires a lesser amount of desorbent

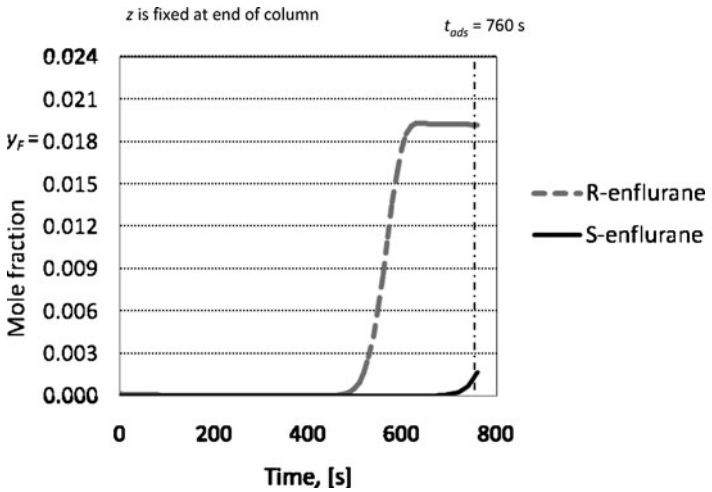

Fig. 9 Mole fraction profiles of *R*- and *S*-enflurane at the end of the column during the adsorption and depressurization steps of a cycle of PSA simulation with operating condition in Table 4. During the adsorption step the outlet mole fraction is collected in the raffinate stream. The two feed mole fractions are again 0.018. The adsorption time is found to be 760 s

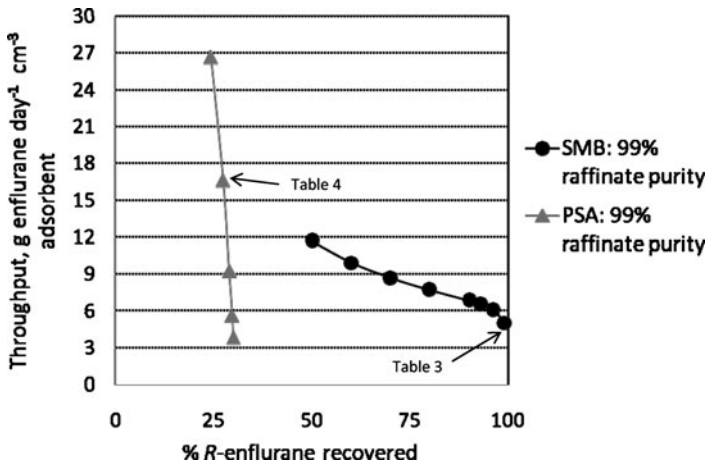

Fig. 10 SMB and PSA optimal throughput values depending on raffinate recovery with 99% raffinate purity as a constraint. The *arrows* point to the values where the operating conditions are reported in Tables 3 and 4 for SMB and PSA respectively

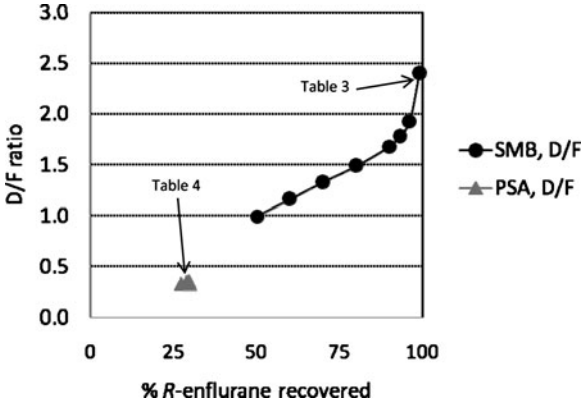

Fig. 11 D/F ratios for SMB and PSA verses % *R*-enflurane recovery. All points correspond to optimal solutions reported in Fig. 10. The *arrows* point to the values where the operating conditions are reported in Tables 3 and 4 for SMB and PSA respectively

for column regeneration due to its stepwise operation. Desorbent is only supplied during the pressurization and purge steps of the process, which constitute less than half of the cycle time. This can be a significant advantage if the product concentration must be high, or desorbent cost cannot be neglected.

The maximized production rate of the SMB was 5.0 g enflurane feed day^{-1} cm^{-3} adsorbent while satisfying a target recovery of 99%, while the maximized product recovery of PSA was 29.9% at a throughput of 3.8 g enflurane feed day^{-1} cm^{-3} adsorbent. These throughput values are far above those in the non-optimized experimental study reported by Biressi et al. (2000, 2002). This result can be attractive for industrial use as it indicates feasible operating conditions where a large amount of purified enfluranes may be produced for pharmacological studies. For further investigation on the feasibility of these processes, the column efficiency must be verified by an experimental study. Furthermore, the poor recovery of PSA may be improved by introducing a modified operating strategy or employing multiple columns while maintaining the high throughput demonstrated in this study.

4 Conclusions and future work

In this work, the resolution of racemic gas mixtures by SMB and PSA is investigated by dynamic simulation and deterministic multi-objective optimization. The concentration profiles and operating conditions at the optimal solutions are investigated and analyzed by dynamic simulation. Furthermore, the trade-off of throughput and target recovery has been investigated systematically. It has been found that the SMB process achieves high recovery which can be as high as 99%, while the recovery using 4-step PSA considered in this work remains relatively low. Nevertheless, the higher throughput of the PSA process can be a significant advantage for inexpensive feed mixtures. Also, the PSA process features a low D/F ratio compared to SMB and this is also economically advantageous if the product concentration must be high or desorbent cost cannot be neglected.

Our future work will extend our optimization strategy to cover a wide variety of different adsorption operations and column configurations. In particular, vacuum swing adsorption (VSA) as well as the SMB process with pressure swing assist proposed by Kostroski and Wankat (2008) will be investigated utilizing our optimization approach. Furthermore, in order to find the optimal column structure from a number of different column configurations, the superstructure approach proposed by Kawajiri and Biegler (2006b) will be applied to this separation problem. These computational studies will be validated by experimental work, where the feed mixture is more highly concentrated and therefore competitive adsorption and non-isothermal behavior must be taken into account for improved model accuracy.

References

Aboul-Enein, H.Y., Abou-Basha, L.I.: The Impact of Stereochemistry on Drug Development and Use. Wiley, New York (1997)

Aboul-Enein, H.Y., Bojarski, J., Szymura-Oleksiak, J.: The impact of chirality of the fluorinated volatile inhalation anesthetics on their clinical applications. Biomed. Chromatogr. **14**, 213–218 (2000)

Biressi, G., Quattrini, F., Juza, M., Mazzotti, M., Shurig, V., Morbidelli, M.: Gas chromatographic simulated moving bed separation of the enantiomers of the inhalation anesthetic enflurane. Chem. Eng. Sci. **55**, 4537–4547 (2000)

Biressi, G., Mazzotti, M., Morbidelli, M.: Experimental investigation of the behavior of gas phase simulated moving beds. J. Chromatogr. A **957**, 211–225 (2002)

Broughton, D.B., Gerhold, C.G.: Continuous sorption process employing fixed bed of sorbent and moving inlets and outlets. U.S. Patent 2985589 (1961)

Cheng, L.S., Wilson, S.T.: Process for separating propylene from propane. U.S. Patent 6293999 (2001)

Dünnebier, G., Klatt, K.U.: Modeling and simulation of nonlinear chromatographic separation processes: a comparison of different modeling approaches. Chem. Eng. Sci. **55**, 373–380 (2000)

Eger II, E.I., Koblin, D.D., Laster, M.J., et al.: Minimum alveolar anesthetic concentration values for the enantiomers of isoflurane differ minimally. Anesth. Analg. **85**, 188–192 (1997)

Ganetsos, G., Barker, P.E.: Preparative and Production Scale Chromatography. Dekker, New York (1993)

Garton, K.J., Yuen, P., Meinwald, J., Thummel, K.E., Kharasch, E.D.: Stereoselective metabolism of enflurane by human liver cytochrome P450 2E1. Drug Metab. Dispos. **23**, 1426–1430 (1995)

Gomes, P.S., Lamia, N., Rodrigues, A.E.: Design of a gas phase simulated moving bed for propane/propylene separation. Chem. Eng. Sci. **64**, 1336–1357 (2009)

Hall, A.C., Lieb, W.R., Franks, N.P.: Stereoselective and non-stereoselective actions of isoflurane on the GABA(A) receptor. Br. J. Pharmacol. **112**, 906–910 (1994)

Harris, B.D., Moody, E.J., Basile, A.S., Skolnick, P.: Volatile anesthetics bidirectionally and stereospecifically modulate ligand binding to GABA receptors. Eur. J. Pharmacol. **267**, 269–274 (1994)

Huang, Q., Malekian, A., Eic, M.: Optimization of PSA process for producing enriched hydrogen from plasma reactor gas. Sep. Purif. Technol. **26**, 22–31 (2008)

Jiang, L., Biegler, L.T., Fox, Grant V: Simulation and optimization of pressure-swing adsorption systems for air separation. AIChE J. **49**, 1140–1157 (2003)

Juza, M., Di Giovanni, O., Biressi, G., Schurig, V., Mazzotti, M., Morbidelli, M.: Continuous enantiomer separation of the volatile inhalation anesthetic enflurane with a gas chromatographic simulated moving bed unit. J. Chromatogr. A **813**, 333–347 (1998)

Kawajiri, Y., Biegler, L.T.: Optimization strategies for simulated moving bed and power feed processes. AIChE J. **52**, 1343–1350 (2006a)

Kawajiri, Y., Biegler, L.T.: Nonlinear programming superstructure for optimal dynamic operations of simulated moving bed processes. Ind. Eng. Chem. Res. **45**, 85 (2006b)

Kawajiri, Y., Biegler, L.T.: Comparison of configurations of a four-column simulated moving bed process by multi-objective optimization. Adsorption **14**, 433–442 (2008)

Ko, D., Siriwardane, R., Biegler, L.T.: Optimization of a pressure-swing adsorption process using zeolite 13X for CO_2 sequestration. Ind. Eng. Chem. Res. **42**, 339–348 (2003)

König, W.A., Krebber, R., Mischnick, P.: Cyclodextrins as chiral stationary phases in capillary gas chromatography, Part V: octakis(3-*O*-butyryl-2,6-di-*O*-pentyl)-γ-cyclodextrin. J. High Resolut. Chromatogr. **12**, 732–738 (1989)

Kostroski, K.P., Wankat, P.C.: Separation of dilute binary gases by simulated moving bed with pressure swing assist: SMB/PSA processes. Ind. Eng. Chem. Res. **47**, 3138–3149 (2008)

LaCava, A., McKeigue, K.: Continuous pressure difference driven adsorption process. U.S. Patent 5487775 (1996)

Li, G., Warner, M., Lang, B.H., Huang, L., Sun, L.S.: Epidemiology of anesthesia-related mortality in the United States, 1999–2005. Anesthesiology **110**, 759–765 (2009)

Meinwald, J., Thompson, W.R., Pearson, D.L., König, W.A., Runge, T., Francke, W.: Inhalational anesthetics stereochemistry: optical resolution of halothane, enflurane, and isoflurane. Science **251**, 560–561 (1991)

Mota, J.P.B., Esteves, I.A.A.C., Eusebio, M.F.J.: Synchronous and asynchronous SMB processes for gas separation. AIChE J. **53**, 1192–1203 (2007)

Nau, C., Strichartz, G.R.: Drug chirality in anesthesia. Anesthesiology **97**, 497–502 (2002)

Nilchan, S., Pantelides, C.C.: On the optimisation of periodic adsorption processes. Adsorption **4**, 113–147 (1998)

Perrut, M.: Advances in supercritical fluid chromatographic processes. J. Chromatogr. A **658**, 293–313 (1994)

Process Systems Enterprise. Optimization Guide. Release v3.2.0. Process Systems Enterprise Limited (2009)

Rao, D.P., Sivakumar, S.V., Mandal, S., Kota, S., Ramaprasad, B.S.G.: Novel simulated moving bed adsorber for the fractionation of gas mixtures. J. Chromatogr. A **1069**, 141–151 (2005)

Ruthven, D.M., Faroq, S., Knaebel, K.: Pressure Swing Adsorption. Wiley, New York (1994)

Schiesser, W.E.: The Numerical Method of Lines: Integration of Partial Differential Equations. Academic Press, San Diego (1991)

Schmidt-Traub, H.: Preparative Chromatography. Wiley, Weinheim (2005)

Storti, G., Mazzotti, M., Furlan, L.T., Morbidelli, M., Carra, S.: Performance of a six port simulated moving bed pilot plant for vapor phase adsorption separations. Sep. Sci. Technol. **27**, 1889–1916 (1992)

Zhang, Z.Y., Mazzotti, M., Morbidelli, M.: Continuous chromatographic processes with a small number of columns: comparison of simulated moving bed with varicol, PowerFeed and ModiCon. Kor. J. Chem. Eng. **21**, 454–464 (2004)